Computational Analysis of Raindrop Radar Reflectivity and Radar Cross Section across Various Frequency Bands

T. Y. Ojebisi[1]*, J.S. Ojo[2], E.O. Olurotimi[3], and M.O Ajewole[2]

[1]Department of Physics, Bamidele Olumilua University of Education, Science and Technology, Ikere Ekiti ,Ekiti State Nigeria
[2]Department of Physics, Federal University of Technology, Akure, Ondo State, Nigeria.
[3]Department of Electronic and Computer Engineering. Durban University of Technology, South Africa
*Corresponding author email: temitopekoladeoje@gmail.com

Abstract This study presents a numerical investigation of radar cross-section (RCS) and radar reflectivity of raindrops using a modified generalized T-matrix method to model realistic non-spheroidal raindrop shapes. The RCS and reflectivity are computed across a range of frequencies for raindrops with radii between 0.25 mm and 4 mm. Results indicate that RCS increases with both raindrop size and frequency when the drop size is smaller than the wavelength. Reflectivity for individual raindrops remains constant for drop radii up to 2 mm, beyond which it gradually increases, reaching a peak at 4 mm. This trend highlights the dependence of reflectivity on raindrop size and shape, especially as drops transition from spherical to oblate forms. At higher frequencies, notably above 60 GHz, the RCS and reflectivity curves exhibit pronounced instability, particularly at 200 GHz, where the wavelength approximates typical raindrop diameters (~1.5 mm). This frequency dependence offers valuable insights into radar system design and application in meteorological forecasting, hydrological modeling, climate studies, and communication system design, where precise rainfall estimation is critical. This theoretical analysis of RCS and reflectivity characteristics thus enhances our understanding of their behavior across frequency ranges and their implications for diverse practical applications.

Keywords: raindrop radar reflectivity, radar cross section, frequency bands, computational analysis, meteorology, radar systems

1. Introduction

Rainfall monitoring and estimation are essential for various applications in meteorology, hydrology, and climate research. Radar systems play a critical role in providing valuable data for these purposes, with raindrop radar reflectivity and radar cross-section (RCS) serving as fundamental parameters in radar observations [1]. Raindrop radar reflectivity quantifies the power returned to the radar receiver from precipitation particles, offering insights into rainfall intensity and distribution [2]. On the other hand, RCS measures the scattering efficiency of targets to radar waves and is crucial for understanding the interaction between radar signals and precipitation particles [3]. The behavior of raindrop radar reflectivity and RCS varies across different frequency bands, and is influenced by factors such as raindrop size distribution, shape, and the dielectric properties of water. Higher frequency radar systems are more sensitive to smaller raindrops, while lower frequency systems may penetrate deeper into precipitation systems but with lower resolution

I. Adimula et al. (eds.), *Proceedings of the 8th URSI-NG Annual Conference (URSI-NG 2024)*, Advances in Physics Research 12,
https://doi.org/10.2991/978-94-6463-644-4_12

[4]. Understanding how raindrop radar reflectivity and RCS change with frequency is essential for optimizing radar systems for accurate rainfall estimation and forecasting.

In this paper, a computational analysis of raindrop radar reflectivity and RCS across various frequency bands is carried out using theoretical models and numerical simulations, the study aims to investigate the behavior of these parameters and their dependence on frequency. The research presented here advances our knowledge of the frequency-dependent properties of raindrop radar reflectivity and RCS, offering important new perspectives for the design of radar systems and meteorological applications.

.

2 Numerical Simulation of Radar Cross- Section of Raindrop

Back scattering of the radar signal, also defined by the radar cross section, strongly depends on the drop shape [5]. The radar cross section (RCS) is the area that intercepts a certain amount of power in the incident beam. It represents the ratio of the power scattered back to the radar receiver by the target to the incident radar power density per unit solid angle on the target, assuming the radiation is isotropic. It is expressed as [6]:

$$\sigma = \frac{4\pi r^2 S_s}{S_i} \tag{1}$$

where S_i is the power density incident at the target, S_s is the scattered power density seen at a distance r away from a target

The RCS of raindrops is usually calculated using different methods, such as the Mie theory for spherical raindrops, expressed as [7]:

$$\sigma = \frac{\lambda}{2\pi r^3} \left| \sum_{n=1}^{\infty} (-1)^n (2n+1)\,(a_n + b_n) \right|^2 \tag{2}$$

For Rayleigh scatterers, the radar cross section is expressed as [8]:

$$\sigma = \frac{\pi^5}{\lambda^4} |K_m|^2 D^6 \tag{3}$$

where $|K_m|$ is a function of the scatterer's refractive index and D is the scatter's diameter.

RCS is estimated for non-spherical raindrops (Pruppacher-Pitter droplets) utilising rigorous approaches such as moment methods, point matching techniques, and the extended boundary condition (EBCM) or T matrix method.

The RCS for singular drops in the T matrix approach is given as a function of the extinction cross section as:

$$\sigma = \sqrt{4\pi\sigma_{ext}} \tag{4}$$

where σ_{ext} is the extinction cross section obtained from the T matrix method[9].

For a rain field medium with drop size distribution $N(D)$, the RCS is expressed as:

$$RCS = \int_0^{\infty} |S|^2 N(D) \tag{5}$$

where $|S|^2$ is the scattering matrix; $N(D)$ is the drop size distribution.

The S-matrix is related to the T-matrix (transition matrix). In many cases, the T-matrix can be used to determine the elements of the S-matrix, which provides information about how the object scatters incident waves at different frequencies. [10]

3 Computation of Raindrop Radar Reflectivity

An object's radar cross section that can be detected by weather radar is measured using the radar reflectivity (Z). It is the amount of power reflected by hydrometeors like raindrops [11]. It refers to the property of a medium or target to reflect incident electromagnetic waves back to the radar system. It is quantified as the total reflecting area of small particles per cubic meter, where these particles possess a dielectric constant greater than zero.

The radar reflectivity is calculated using:

$$Z = \frac{\lambda^4}{\pi^5|k_w|^2}\int_0^\infty |S|^2 N(D) \quad (6)$$

where S is the scattering matrix , λ is the wavelength, $N(D)$ is the drop size distribution, and k_w is the dielectric factor expressed as a function of refractive index of water as :

$$k_w = \frac{(m_w^2-1)}{(m_w^2+2)} \quad (7)$$

m_w is the refractive index of water

The lognormal distribution of the form [12-13]:

$$N(D) = \frac{N_T}{\sigma D\sqrt{2\pi}} \exp\left[-\frac{1}{2}\left\{\frac{In(D)-\mu}{\sigma}\right\}^2\right] \quad (8)$$

where N_T is the total number of raindrops of all sizes, μ is the mean of $\text{In}(D)$, σ is the standard deviation.

4. Results and Discussion

This study has numerically investigated the radar cross section and radar reflectivity of raindrops using the modified generalized T-matrix method to account for the non-spheroidal realistic raindrop [14-16]. The radar cross section and radar reflectivity at some selected frequencies for raindrops of radius 0.25 mm to 4 mm. were computed and are presented in Figure 1(a-c) and Figure 2(a-b), respectively.

Radar cross section increases with increasing drop size and frequency when the drop size is smaller than the wavelength. Single-drop reflectivity has constant values for all drops up to 2 mm radius and increases gradually until it reaches a maximum at 4 mm radius. This demonstrates that as the drop size grows and deviates from the spherical shape to the oblate form, the reflectivity increases, indicating the dependency of reflectivity on raindrop shape and size. For drops with a radius up to 2 mm, reflectivity is essentially stable because the scattering properties of these smaller drops do not vary significantly. This stability means that reflectivity values for these drops can serve as a baseline or reference in predictive models. When drop size increases beyond this threshold, the interaction with electromagnetic waves intensifies, causing the reflectivity to change due to more complex scattering effects.

At higher frequencies, particularly above 60 GHz, both radar reflectivity and cross-section patterns show increased instability, with the most pronounced fluctuations occurring around 200 GHz. This behavior is due to the wavelength, approximately 1.5 mm at these frequencies, closely matching the size of raindrops. This size-wavelength alignment enhances complex scattering interactions, resulting in the observed instability in reflectivity and cross-section values at these high frequencies

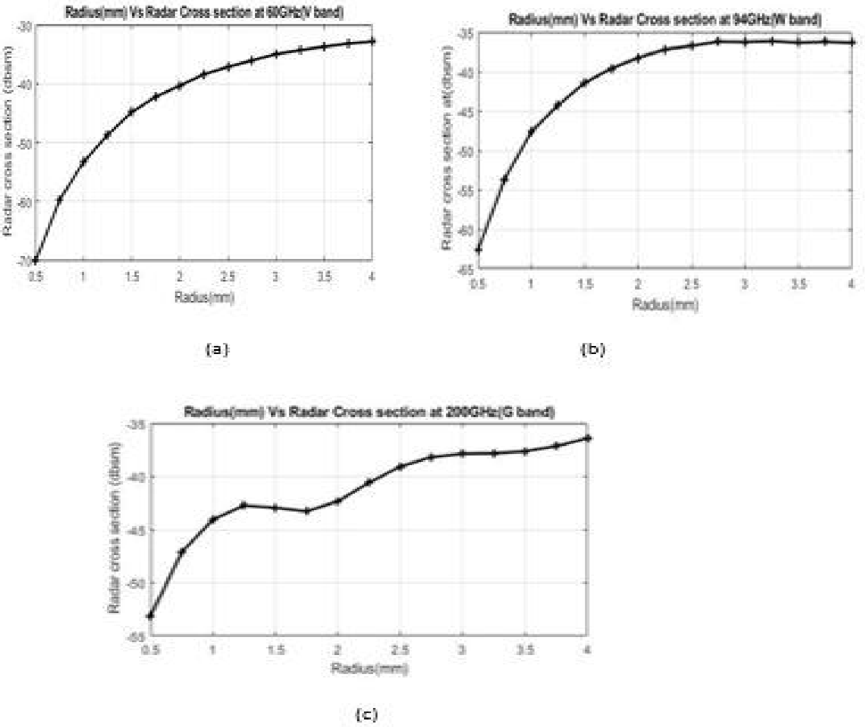

Figure 1: Radar cross section against drop radius at 60 GHz (b) at 94 GHz (c) at 200 GHz

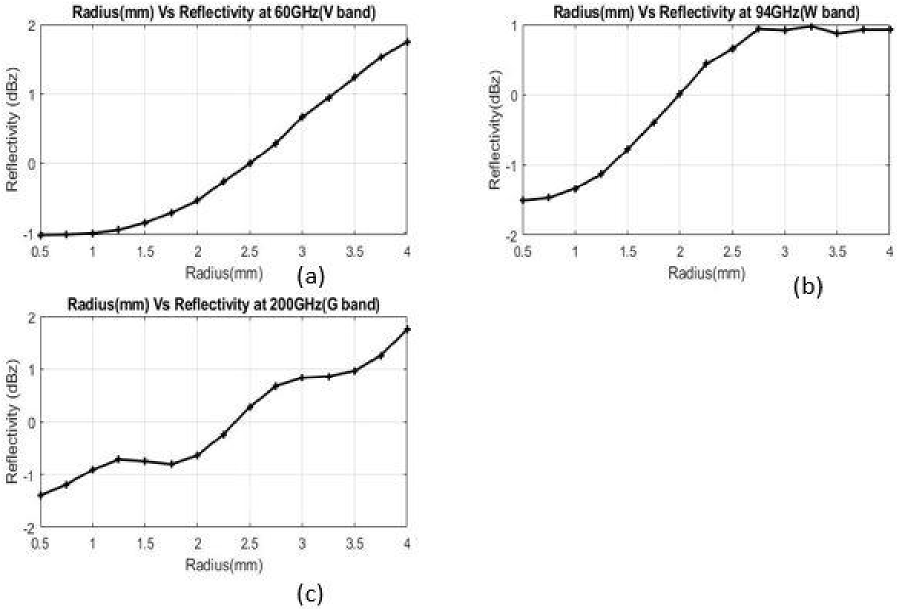

Figure 2: Radar reflectivity against drop radius at 60 GHz (b) at 94 GHz (c) at 200 GHz

4.1 Variation of Radar Reflectivity and Cross Section with Frequency

The variation of the radar cross sections and radar reflectivity with frequency was examined at various frequencies bands in the range of X band to the G band, as shown in Figures 3 and 4 respectively

The radar cross section shown in Figure 3. Increases with increasing drop size when the drop size is smaller than the wavelength, and similar irregularities are observed when the drop size becomes comparable with the wavelength. However, at higher frequencies, when the wavelength becomes smaller than the drop sizes, a reduction in the radar cross section is observed. This implies that an increase in the frequency of waves propagated through a rain medium characterized by larger raindrops would result in increased absorption and scattering as long as the drop radius is less than the wave wavelength.

Figure 4 shows the single drop reflectivity at various raindrops. This plot reveals that reflectivity decreases with increasing frequency and approaches zero in the high frequency band. This is consistent with the well-known fact that when a wave's frequency increases, its wavelength decreases, reflectivity declines, and absorption increases.

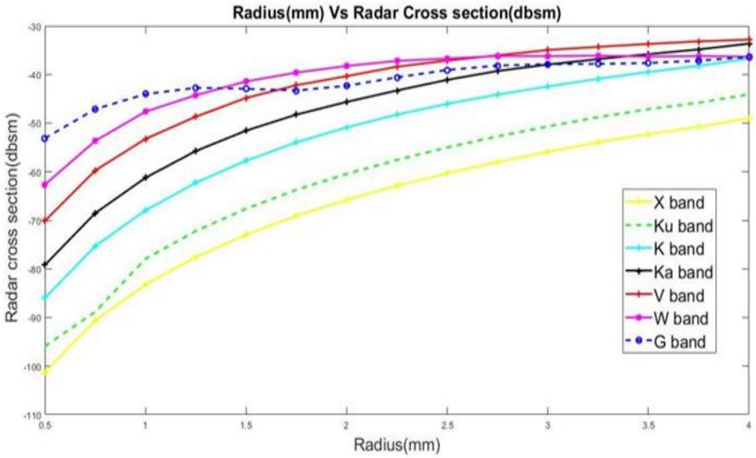

Figure 3: Variation of Radar Cross Section with Frequency

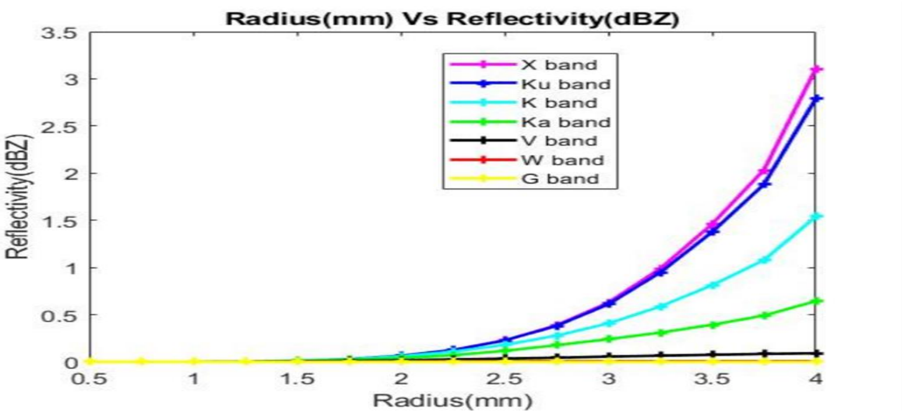

Figure 4: Variation of Radar Reflectivity with Frequency

5. Conclusion and recommendation

The T-matrix technique was employed to compute the radar cross section from each asymmetric raindrop, and it was discovered that radar cross section is drop size as well as frequency dependent, with the higher frequency band showing the most fluctuation.

The reflectivity of raindrops was also computed using the lognormal distribution, and variations in raindrop radar reflectivity and RCS across different frequency bands were also observed. These variations are influenced by factors such as raindrop size distribution, shape, and the dielectric properties of water. Understanding these frequency-dependent characteristics is crucial for optimizing radar systems for meteorological applications, including rainfall estimation and forecasting. This study is also significant in the field of communication systems, particularly for microwave and millimeter-wave bands that are highly sensitive to atmospheric conditions, by analyzing raindrop radar reflectivity and radar cross-section, this study provides critical insights into how raindrop size distributions and rainfall intensities affect signal attenuation and scattering. These insights enable telecommunication networks to better predict and mitigate signal degradation due to rainfall, thereby enhancing link reliability during adverse weather conditions. Furthermore, an understanding of frequency-dependent radar cross-sections supports the design of communication systems that are optimized for specific environmental conditions, facilitating frequency selection or adaptation strategies to reduce rain-induced losses. Finally, this study contributes to the calibration and performance evaluation of weather radars, which are essential for real-time monitoring and forecasting, thus indirectly supporting communication planning and operations by providing accurate, location-specific rainfall data.

Reference

[1] Bringi, V. N., & Chandrasekar, V. (2001). Polarimetric Doppler Weather Radar: Principles and Applications. Cambridge University Press.

[2] Battan, L. J. (1973). Radar Observations of Rain. Annual Review of Earth and Planetary Sciences, 1(1), 303-338.

[3] Ulaby, F. T., Moore, R. K., & Fung, A. K. (2014). Microwave Remote Sensing: Active and Passive: Volume I: Microwave Remote Sensing Fundamentals and Radiometry (Vol. 1). Artech House.

[4] Doviak, R. J., & Zrnić, D. S. (2006). Doppler Radar and Weather Observations. Academic Press.

[5] Veselovska, G. B., and Khlopov, G. I. (2015). Radar cross section of non-spherical raindrops. *Telecommunications and Radio Engineering*, *74*(12), 1085-1097.

[6] Skolnik, M. I. (2008). Introduction to Radar Systems (3rd ed.). McGraw-Hill

[7] Matzler, C. (2002). Drop-size distributions and Mie computation. IAP Research Report 2002-16, University of Bern, Bern.

[8] Bodine, D. (2014). Polarimetric radar observations and numerical simulations of tornadic debris.

[9] Kolade-Oje, T. Y., Ajewole, M. O., Ojo, J. S., & Adediji, A. T. (2022). Computation of spherical and non-spherical raindrop scattering parameters using the Mie and T-matrix models in relation to 5G wireless systems. *The European Physical Journal Plus*, *137*(6), 1-9.

[10] Somerville, W. R. C., Auguié, B., and Le Ru, E. C. (2016). SMARTIES: User-friendly codes for fast and accurate calculations of light scattering by spheroids. *Journal of Quantitative Spectroscopy and Radiative Transfer*, 174, 39-55.

[11] Falconi, M. T. (2018). Remote sensing and electromagnetic modeling applied to weather and forward scatter radar. *Doctoral Sapienza University of Rome*.

[12] Adetan, O., & Afullo, T. J. (2014). Raindrop size distribution and rainfall attenuation modeling in equatorial and subtropical Africa: the critical diameters. Annals of telecommunications-annales des telecommunications, 69, 607-619.

[13] Sumbiri, I. A., & Afullo, T. J. (2017). Optimized raindrop size distribution model for equatorial Africa using measurements in Butare, Rwanda. *IEEE Transactions on Antennas and Propagation*, 65(5), 2147-2157. doi:10.1109/TAP.2017.2688464

[14] Kolade-Oje, T. Y., Ajewole, M. O., Ojo, J. S., & Adediji, A. T. (2021, October). Simulation of raindrop shapes and its interaction with electromagnetic wave. In Journal of Physics: Conference Series (Vol. 2034, No. 1, p. 012015). IOP Publishing.
[15] Beard, K. V., and Chuang, C. (1987). A New Model for the Equilibrium Shape of Raindrops. Journal of the Atmospheric sciences, 44(11), 1509-1524.
[16] Pruppacher, H. R., and Pitter, R. L. (1971). A semi-empirical determination of the shape of cloud and rain drops. Journal of Atmospheric Sciences, 28(1), 86-94. Quant. Spectrosc. Radiat. Trans. 174, 39–55 (2016)